

## Collateral sensitivity is contingent on the repeatability of evolution

Daniel Nichol<sup>1,2,†,\*</sup>, Joseph Rutter<sup>3</sup>, Christopher Bryant<sup>4</sup>, Andrea M Hujer<sup>3, 4</sup>, Sai Lek<sup>5</sup>, Mark D Adams<sup>5</sup>, Peter Jeavons<sup>1</sup>, Alexander RA Anderson<sup>2</sup>, Robert A Bonomo<sup>3,4,6,7,8,9</sup>, Jacob G Scott<sup>7,10,11\*</sup>

**1 Department of Computer Science, University of Oxford, Oxford, UK**

**2 Department of Integrated Mathematical Oncology, H. Lee Moffitt Cancer Center and Research Institute, Tampa, FL, USA**

**3 Research Service, Louis Stokes Department of Veterans Affairs Hospital, Cleveland, OH, USA**

**4 Department of Medicine, Case Western Reserve University School of Medicine, Cleveland, OH, USA**

**5 The Jackson Laboratory for Genomic Medicine, 10 Discovery Dr, Farmington, CT, USA**

**6 Departments of Biochemistry, Molecular Biology and Microbiology, and Pharmacology, Case Western Reserve University School of Medicine, Cleveland, OH, USA**

**7 Center for Proteomics and Bioinformatics, Case Western Reserve University School of Medicine, Cleveland, OH, USA**

**8 Medicine Service and Geriatric Research Education and Clinical Center (GRECC), Louis Stokes Cleveland Department of Veterans Affairs Medical Center, Cleveland, OH, USA**

**9 CARES, CWRU-VA Center for Antibiotic Resistance and Epidemiology, Cleveland, OH, USA**

**10 Wolfson Centre for Mathematical Biology, Mathematical Institute, University of Oxford, Oxford, UK**

**11 Departments of Translational Hematology and Oncology Research and Radiation Oncology, Cleveland Clinic, Cleveland, OH, USA**

**† Present address: Centre for Evolution and Cancer, Institute of Cancer Research, London, UK**

**\* daniel.nichol@icr.ac.uk (DN); scottj10@ccf.org (JGS)**

1

## 2 **Abstract**

3       Antibiotic resistance represents a growing health crisis that necessitates the immediate  
4 discovery of novel treatment strategies. One such strategy is the identification of sequences  
5 of drugs exhibiting *collateral sensitivity*, wherein the evolution of resistance to a first drug  
6 renders a population more susceptible to a second. Here, we demonstrate that sequential multi-  
7 drug therapies derived from *in vitro* evolution experiments can, in some cases, have overstated  
8 therapeutic benefit – potentially suggesting a collaterally sensitive response where cross resistance  
9 ultimately occurs. The evolution of drug resistance need not be genetically or phenotypically  
10 convergent, and where resistance arises through divergent mechanisms, the efficacy of a second  
11 drug can vary substantially. We first quantify the likelihood of this occurring by use of a  
12 mathematical model parametrised by a set of small combinatorially complete fitness landscapes  
13 for *Escherichia coli*. We then verify, through *in vitro* experimental evolution, that a second-line  
14 drug can indeed stochastically exhibit either increased susceptibility or increased resistance when  
15 following a first. Genetic divergence is confirmed as the driver of this differential response through  
16 targeted and whole genome sequencing. These results indicate that the present methodology  
17 of designing drug regimens through experimental collateral sensitivity analysis may be flawed  
18 under certain ecological conditions. Further, these results suggest the need for a more rigorous  
19 probabilistic understanding of the contingencies that can arise during the evolution of drug  
20 resistance.

21 The emergence of drug resistance is governed by Darwinian dynamics, wherein resistant  
22 mutants arise stochastically in a population and expand under the selective pressure of therapy [29].  
23 These evolutionary principles underpin resistance to the presently most effective therapies for  
24 bacterial infections [6], cancers [12], viral infections [4] and disparate problems such as the  
25 management of invasive species and agricultural pests [19]. Biological mechanisms of drug  
26 resistance often carry a fitness cost in the absence of the drug and further, different resistance  
27 mechanisms can interact with one another to produce non-additive fitness effects, a phenomenon  
28 known as epistasis [26]. These trade-offs can induce rugged fitness landscapes, potentially  
29 restricting the number of accessible evolutionary trajectories to high fitness [27, 36] or rendering  
30 evolution irreversible [32].

31 Identifying evolutionary trade-offs forms the basis of an emerging strategy for combating  
32 drug resistance; prescribing sequences of drugs wherein the evolution of resistance to the first  
33 induces susceptibility to the next [11, 14, 16, 23]. Where this occurs, the first drug is said to  
34 induce *collateral sensitivity* in the second. Conversely, where the first drug induces increased  
35 resistance in the second, *collateral* (or *cross*) *resistance* has occurred. Recently, *in vitro* evolution  
36 experiments have been performed, in both bacteria [7, 14, 18, 22, 31, 33] and cancers [9, 40], to  
37 identify drug pairs or sequences exhibiting collateral sensitivity. Frequently, these experiments  
38 proceed by culturing a population in increasing concentrations of a drug to induce resistance, and  
39 then assaying the susceptibility of the resultant population to a panel of potential second-line  
40 therapies. From these experiments, sequences or cycles of drugs in which each induces collateral  
41 sensitivity in the next have been suggested as potential therapeutic strategies to extend the  
42 therapeutic efficacy of a limited pool of drugs [9, 14]. For some cancer therapies, which often  
43 have severe side-effects and high toxicity, such sequential therapies may be the only way to  
44 combine the use of multiple drugs.

45 Drug pairs that are identified as collaterally sensitive in a small number of *in vitro* evolutionary  
46 replicates may not in fact induce collateral sensitivity each time they are applied. This hypothesis  
47 arises from the observation that evolution is not necessarily repeatable; resistance to a drug can  
48 arise through multiple different mechanisms, as has been observed in cancers [38] and bacteria [3].  
49 Further, one mechanism may confer resistance to a second drug, whilst another may induce  
50 increased susceptibility, as was recently demonstrated in a drug screen of over 3000 strains of  
51 *Staphylococcus aureus* [15]. In previous experimental evolution studies to identify collateral  
52 sensitivity this phenomenon has been directly observed. For example, Barbosa et al. [2] observed  
53 contrasting collateral response in evolutionary replicates of *Pseudomonas aeruginosa*. Oz et al. [24]  
54 observed the same phenomenon in *E. coli* wherein a pair of evolutionary replicates was performed  
55 under exposure to the ribosomal (30S) inhibitor tobramycin, resulting in one exhibiting increased  
56 sensitivity to chloramphenicol and one exhibiting increased resistance. Similar effects are evident

57 in cancer studies. Zhao et al. [40] observed that the sensitivity of a BCR-ABL leukaemia cell line  
58 to cabozantinib can both increase and decrease following exposure to bosutinib, and identified a  
59 single nucleotide variation responsible for this differential collateral response.

60 The extent of the impact of differential collateral response on the design of sequential drug  
61 therapies is not yet fully understood. Here, we provide a clear evolutionary explanation for  
62 differential patterns of collateral response through a combination of mathematical modelling  
63 and experimental evolution. Through mathematical modelling we demonstrate the extent to  
64 which the existence of multiple evolutionary trajectories to drug resistance can render collateral  
65 sensitivities stochastic, and discuss the implications for *in vitro* experimental evolution. We  
66 next empirically demonstrate the existence of multiple trajectories in the evolution of *E. coli*  
67 through *in vitro* experimental evolution. Previous studies have explored the collateral response  
68 by considering all pairs from a pool of antibiotics, each with a small number of evolutionary  
69 replicates [14, 18, 31, 33]. We instead perform 60 parallel evolutionary replicates of *E. coli*  
70 under cefotaxime to demonstrate the extent of heterogeneity in second line drug sensitivity.  
71 Through genomic sequencing we confirm that different mutations (i.e. different evolutionary  
72 trajectories) are responsible for this heterogeneity. Critically, we find that collateral sensitivity is  
73 never universal, and is in fact rare. Finally, we derive *collateral sensitivity likelihoods* which we  
74 argue are critical statistical benchmarks for the clinical translation of sequential drug therapies.

75

## 76 Results

77

### 78 Mathematical Modelling of Evolution

79 The potential impact of divergent evolution can be conceptualised in the classical fitness  
80 landscape model of Wright [37], wherein genotypes are projected onto the two dimensional  $x - y$   
81 plane and fitness represented as the height above this plane. Evolution can be viewed as a  
82 stochastic ‘up-hill’ walk in this landscape wherein divergence can occur at a saddle. Figure 1  
83 shows such a schematic fitness landscape annotated to demonstrate the capacity for divergent  
84 evolution and the potential effects on collateral sensitivity.

85 Previous studies have attempted to empirically determine the structure of the fitness landscape  
86 for a number of organisms and under different drugs [8]. In these studies, a small number of  
87 mutations associated with resistance are first identified. Strains are engineered corresponding  
88 to all possible combinations of presence and absence of these mutations and the fitness of each  
89 strain is measured by a proxy value, for example minimum inhibitory concentration (MIC) of a  
90 drug or average growth rate under a specific dose. These measurements are combined with the



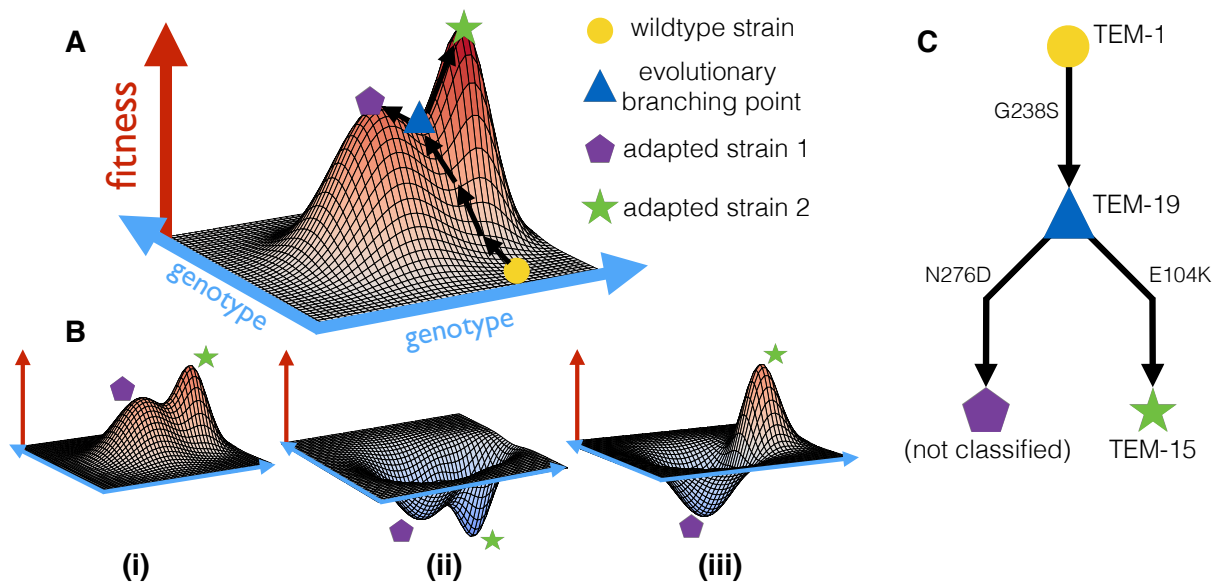


**Figure 1. Evolutionary saddle points can drive divergent collateral response.** **A)** A schematic fitness landscape model in which divergent evolution can occur. Following Wright [37], the  $x - y$  plane represents the genotypes and the height of the landscape above this plane represents fitness. Two evolutionary trajectories, both starting from a wild-type genotype (yellow circle), are shown. These trajectories diverge at an evolutionary saddle point (blue triangle) and terminate at distinct local optima of fitness (purple pentagon, green star). As the saddle point exists, evolutionary trajectories need not be repeatable. **B)** Schematic landscapes for a potential follow-up drug are shown, the collateral response can be (i) always cross-resistant, (ii) always collaterally sensitive or (iii) dependent on the evolutionary trajectory that occurs stochastically under the first drug. **C)** A potential evolutionary branching point in the TEM gene of *E. coli* identified in the fitness landscape for cefotaxime derived by Mira et al. [21].

91 known genotypes to form a fitness landscape. However, to derive fitness landscapes through this  
92 method, the number of strains that must be engineered grows exponentially with the number of  
93 mutations of interest. Thus only small, combinatorially complete, portions of the true fitness  
94 landscape can be measured, for example consisting of 2-5 alleles [8, 25, 36]. Nevertheless, these  
95 restricted fitness landscapes can provide valuable insight into the evolution of drug resistance.

96 Mira et al. [21] derived fitness landscapes for *E. coli* with all combinations of four fitness  
97 conferring mutations (M69L, E104K, G238S and N276D) in the TEM gene and measured fitness  
98 under 15 different  $\beta$ -lactam antibiotics (See Figure S1), using the average growth rate (over 12  
99 replicates) as a proxy of fitness. Of these 15 landscapes, 14 were identified as having multiple  
100 local optima of fitness, indicating the potential for the divergence of evolutionary trajectories.  
101 We utilised these landscapes, coupled with a previously published mathematical model [23] (see  
102 Methods), to estimate the likelihood of the different evolutionary trajectories from a wild-type

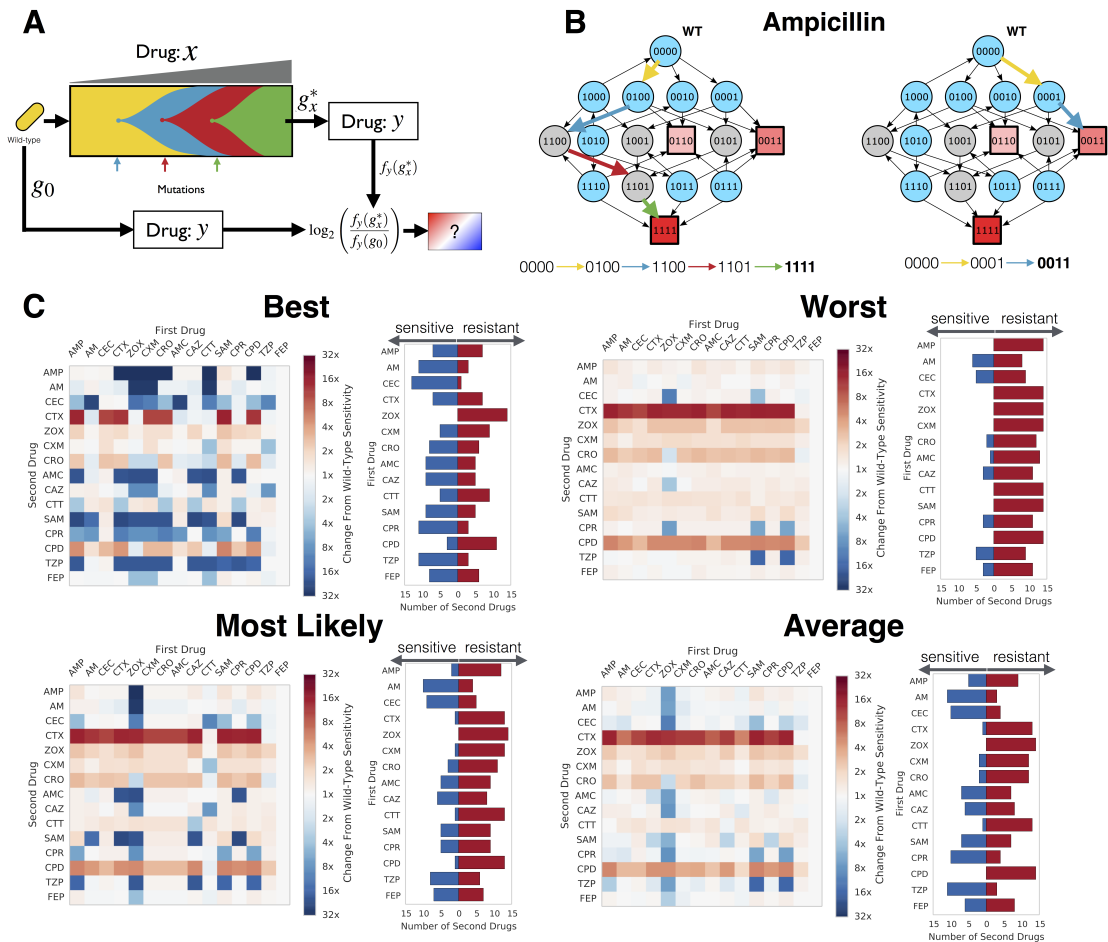


**Figure 2. Mathematical modeling predicts highly variable collateral response. A)** A schematic of the model used to derive collateral response. Sequential mutations are simulated to fix in the population until a local optimum genotype arises. The fitness of this resultant genotype is compared to the fitness of the wild-type genotype for each of the panel of antibiotics. **B)** The landscape for ampicillin derived by Mira et al. [21] represented as a graph of genotypes. Arrows indicate fitness conferring mutations between genotypes represented as nodes. Cyan nodes indicate genotypes from which evolution can stochastically diverge, grey nodes indicate genotypes from which there is only a single fitness conferring mutation. Squares indicate local optima of fitness with colour indicating the ordering of fitness amongst these optima (darker red indicates higher fitness). Two divergent evolutionary trajectories, in the sense of the model shown schematically in **A**, are highlighted by coloured arrows. **C)** The best, worst, most likely and mean tables of collateral response derived through stochastic simulation of the experimental protocol. Columns indicate the drug landscape under which the simulation was performed and rows indicate the follow-up drug under which the fold-change from wild-type susceptibility is calculated. Bar charts indicate, for each labelled first drug, the number of follow-up drugs exhibiting collateral sensitivity (blue) or cross resistance (red) in each case.

Antibiotic	Abbreviation	Antibiotic Group	Notes
Cefotaxime	CTX	Cephalosporin	
Ciprofloxacin	CIP	Fluoroquinolone	
Ampicillin/Sulbactam	SAM	$\beta$ -lactam combination	2:1 ratio of ampicillin to sulbactam
Gentamicin	GNT	Aminoglycoside	
Ticarcillin/Clavulanate	TIC	$\beta$ -lactam combination	2 $\mu$ g/ml clavulanate
Phosphomycin	PMC	Phosphomycin	
Ceftolozane/Tazobactam	CFT	$\beta$ -lactam combination	2:1 ratio of ceftolozane to tazobactam
Piperacillin	PIP	Penicillin	
Cefazolin	CFZ	Cephalosporin	

**Table 1. Antibiotic drugs used in this study.**

103 genotype (denoted 0000) to each of the fitness optima. Using this model, we performed *in*  
104 *silico* assays for collateral sensitivity, mirroring the approach taken Imamovic and Sommer [14]  
105 (Figure 2). For each drug, we first stochastically simulated an evolutionary trajectory from  
106 the wild-type genotype to a local fitness optimum genotype and then, for all other landscapes,  
107 compared the fitness of this local optimum genotype to that of the wild-type. A schematic  
108 of this simulation is shown in Figure 2(A). Figure 2(B) shows an example of two evolutionary  
109 trajectories that can arise stochastically in this model under the fitness landscape for ampicillin.

110 We exhaustively enumerated all tables of collateral response that can arise under this model  
111 (See Figures S2-S10 for further details). Figure 2(C) shows the best case (most susceptible  
112 following evolution), worst case (highest resistance following evolution) and mostly likely collateral  
113 response tables that arose in this analysis, along with the mean collateral response table  
114 (expectation of collateral response for each pair). This analysis suggests that there is remarkable  
115 variation in collateral response arising solely from the stochastic nature of mutation that ultimately  
116 drives evolution under a first drug. Indeed, we find a total of 82,944 unique tables can arise,  
117 of which the most likely occurs with probability 0.0023. Amongst the 225 ordered drug pairs,  
118 only 28 show a guaranteed pattern of collateral sensitivity, whilst a further 94 show a pattern of  
119 guaranteed cross resistance. For 88 pairs, the first drug can induce either collateral sensitivity or  
120 cross resistance in the second as a result of divergent evolution under the first drug. Critically,  
121 if a collateral response table is generated by stochastic *in silico* simulation of the methodology  
122 of Imamovic and Sommer [14], and a collaterally sensitive drug pair chosen at random from this  
123 table, then the expected probability that first of these two drugs will induce cross resistance in  
124 the second is 0.513 (determined from  $10^6$  simulations of this process).

125

## 126 **Experimental Evolution Induces Heterogeneous Collateral Response**

127 The mathematical model used above represents a simplification of biological reality as the  
128 assumption of a monomorphic population need not hold and the parametrisation is made using

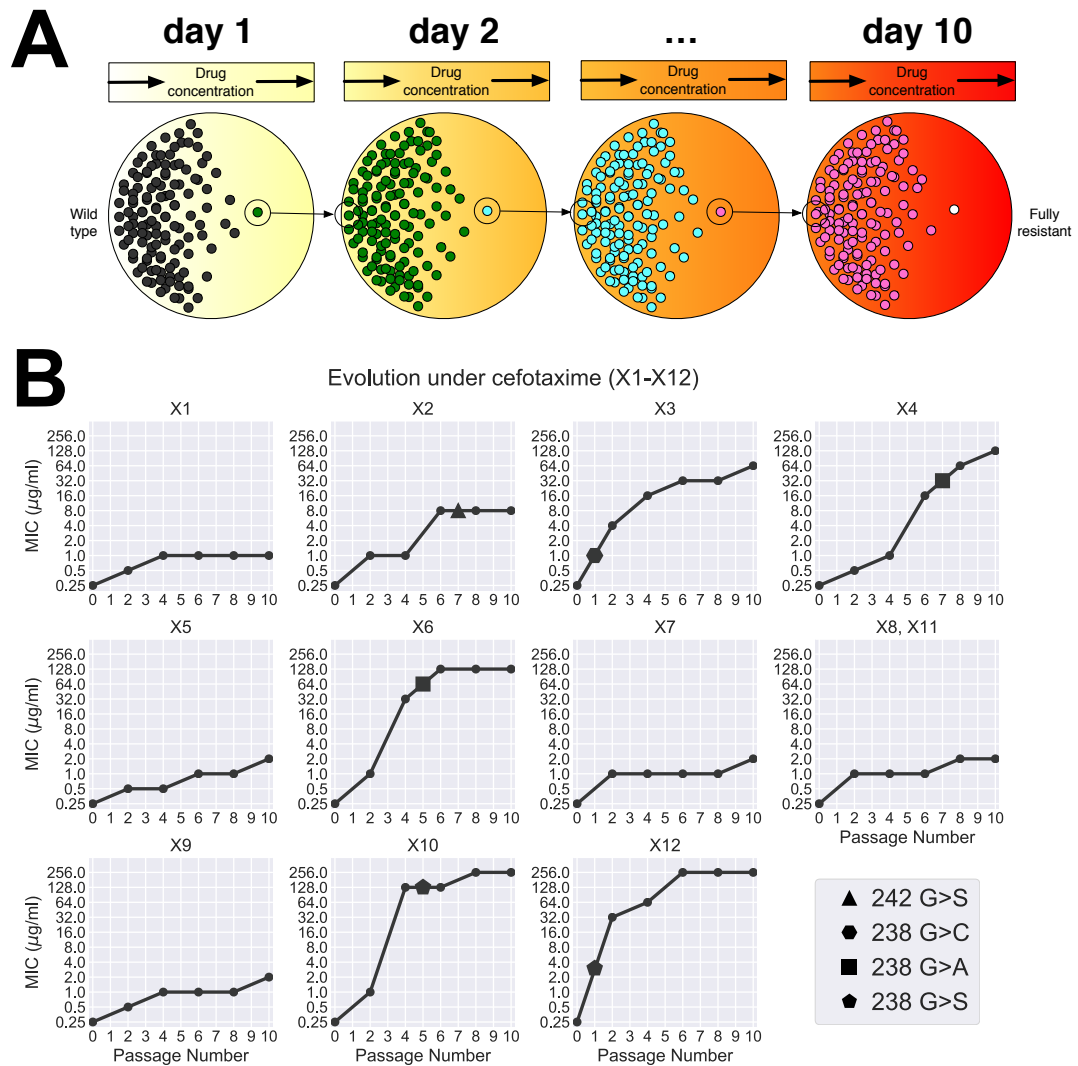


**Figure 3. Experimental evolution reveals divergent collateral response.** **A)** A schematic of the evolutionary experiment. *E. coli* were grown using the gradient plate method and passaged every 24 hours for a total of 10 passages. Sixty replicates of experimental evolution were performed. **B)** The MIC for 12 replicates (X1-X12) under cefotaxime exposure was measured following passages 0, 2, 4, 6, 8 and 10. These values are plotted, revealing heterogeneity in the degree of resistance evolved to cefotaxime. Targeted sequencing of the SHV gene was performed following each passage revealing four different SNVs between the replicates. Geometric shapes indicate these mutations at the earliest time point they were detected in each replicate.

129 incomplete fitness landscapes. To experimentally validate our predictions, we verified the existence  
130 of divergent collateral response through experimental evolution. Mirroring previous experimental  
131 approaches [7, 9, 14, 22, 40], we performed *in vitro* evolution of *E. coli* (strain IDH10B carrying  
132 phagemid pBC SK(-) 198, expressing the *beta*-lactamase gene SHV-1) in the presence of the  
133  $\beta$ -lactam antibiotic cefotaxime. Bacterial populations were grown using the gradient plate  
134 method with concentrations of cefotaxime varying between 0.06  $\mu\text{g}/\text{ml}$  and 256  $\mu\text{g}/\text{m}$  over a course  
135 of 10 passages lasting 24 hours (See Figure 3(A) and Methods for details). In total, 60 replicates  
136 of experimental evolution were performed. We denote the resulting populations by X1-X60.  
137 For replicates X1-X12, aliquots were taken following each second passage and the minimum  
138 inhibitory concentration (MIC) to a panel of second line drugs assayed. A time-series for the  
139 MIC of X1-X12 replicates under cefotaxime is shown in Figure 3(B). As expected, the replicates  
140 exhibit increased resistance to cefotaxime over the 10 passages, although with varying magnitude  
141 and different trajectories.

142 For each of a panel of 8 second-line antibiotics (Table 1), the MIC for the replicates X1-X60 was  
143 determined following passage 10, in addition to the MIC for the parental strain (Supplementary  
144 Table 2, Methods). Figure 4 shows how the MICs of X1-X60 differ from the parental line. As  
145 predicted, we find that the collateral change in sensitivity is highly heterogeneous, and show  
146 that both collateral sensitivity and cross resistance can arise to the antibiotics piperacillin (PIP),  
147 ticarcillin/clavulanate (TCC) and ampicillin/sulbactam (AMS).

148

## 149 Genomic Profiling Reveals Divergent Evolution

150 Differential patterns of drug resistance could be driven by the different replicates having  
151 experienced different numbers of sequential mutations along a single trajectory wherein each  
152 induces a shift in response (temporal collateral sensitivity [40]), by evolutionary divergence at  
153 a branching point in the landscape or by non-genetic mechanisms of resistance. To elucidate  
154 underlying mechanisms, we first performed targeted sequencing of the SHV gene for each of the 10  
155 passage time points for 12 evolutionary replicates (X1-X12) (Figure 3(B)). Through this analysis  
156 we identified five variants of SHV-1 amongst the 12 replicates. X1, X5, X7-X9 and X11 all  
157 possess wild-type SHV-1, X2 possesses the substitution G242S, X3 possesses G238C, X4 and X6  
158 both possess G238A, and X10 and X12 both possess G238S. This analysis revealed no evidence  
159 of double substitutions in SHV, indicating a minimum of four fitness conferring substitutions  
160 that can occur in SHV-1 during exposure to cefotaxime, and confirming the existence of a  
161 multi-dimensional evolutionary branching point in the fitness landscape. Further, the sensitivity  
162 of the population to a second drug appears to be (at least partially) dependent on which of  
163 these substitutions occurs (Figure 3(C)). For example, replicate X3 (harbouring G238C) exhibits  
164 a significant increase in susceptibility to TIC, PIP and SAM, whilst those replicates found to

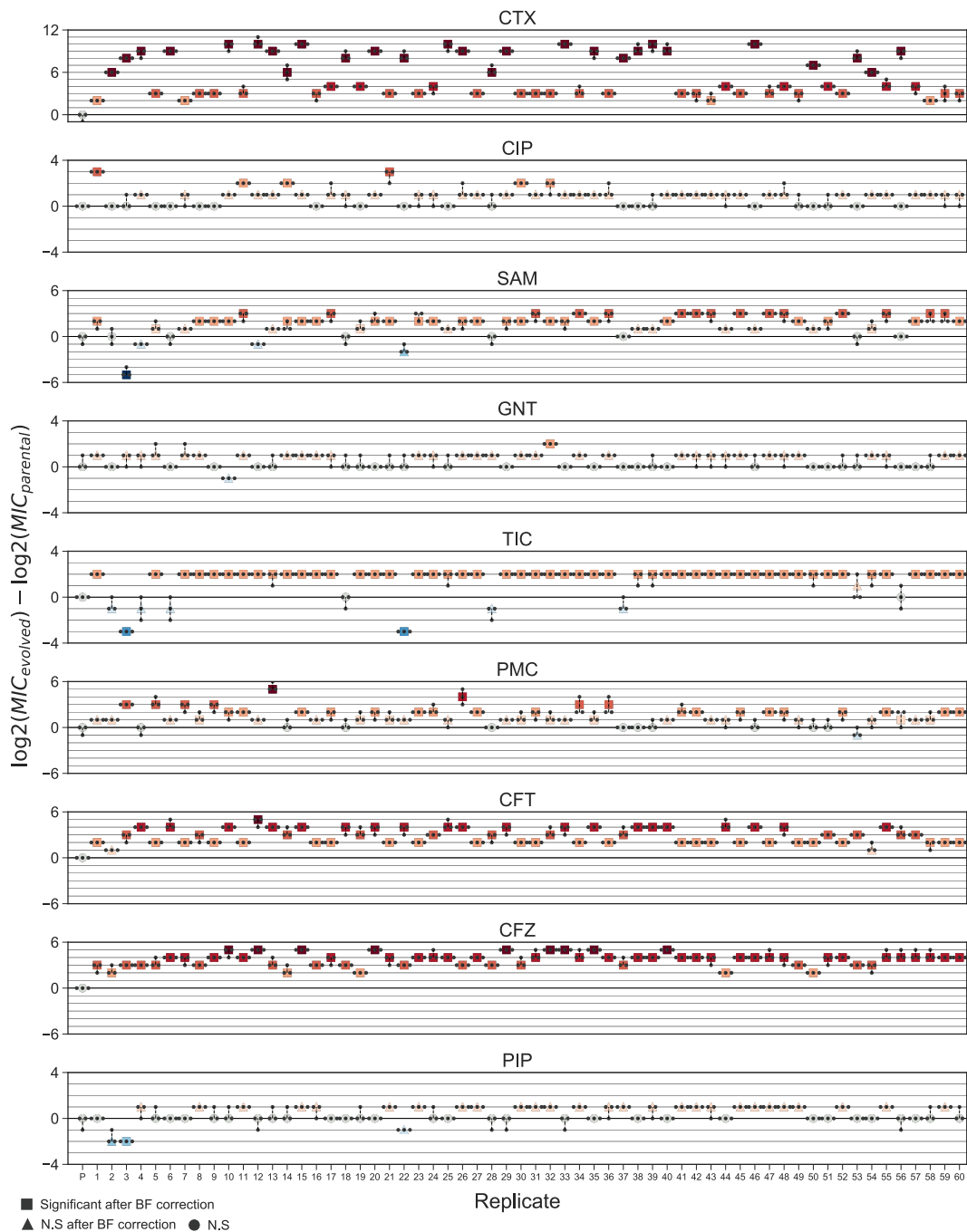


**Figure 4. Collateral response following evolution under cefotaxime.** The maximum likelihood estimates for the MICs of replicates X1-X60 under cefotaxime and eight other antibiotics. Small markers indicate individual measurements (taken in triplicate). Significance is determined via likelihood ratio test and Bonferroni (BF) corrected.

165 harbour wild-type SHV-1, or the other SNVs, exhibit either cross-resistance or no significant  
166 change in susceptibility to these drugs.

167 Through targeted sequencing of SHV alone we cannot not exclude the possibility that  
168 mutations to other genes, or large scale genomic alterations such as insertions or deletions, drive  
169 further divergence in collateral response. To explore whether additional background mutations  
170 arose during selection, we produced draft genome sequences for the replicates X1-X12 after  
171 passage 10 and looked for evidence of additional mutations. This genomic data confirmed the  
172 SHV-1 mutations found by sequencing of PCR products as described above. Nine of the twelve  
173 replicates contained additional mutations that include single-nucleotide variants (SNVs), large  
174 (>5kb) deletions, and replicate-specific sites for insertion of IS1D (Table 2). None of these  
175 were deemed likely to impact cefotaxime resistance as they do not occur in genes known to be  
176 associated with drug resistance. As such, we conclude that mutations in SHV-1 are the primary  
177 drivers of cefotaxime resistance. For example, for replicate X12, which exhibits the highest  
178 endpoint MIC, no additional mutations were detected. In contrast, X1, X5, X8, X9, and X11  
179 all had genomic mutations, lacked SHV-1 variants, and had the lowest final cefotaxime MIC.  
180 Thus, the SHV-1 mutations appear to be the primary factor determining primary resistance. We  
181 excluded the possibility of amplifications of SHV-1 by consideration of read depth ratios. The  
182 ratio of reads mapped to the gene and reads mapped to the plasmid backbone was very similar  
183 across all samples. The ratio of plasmid reads to chromosomal reads did differ across samples,  
184 but the fraction of plasmid-derived reads did not correlate with the MIC for cefotaxime (data  
185 not shown) and is more likely due to variation in extraction efficiency for chromosomal versus  
186 plasmid DNA.

187 We note that X7 exhibits an increase in resistance to cefotaxime without any associated  
188 genomic alterations. Similarly X1, X5, X9 and X12 exhibit mutations, but none that are known  
189 to be associated with antibiotic resistance. Thus, we can infer that physiological adaptation or  
190 epigenetic adaptation is also driving resistance to cefotaxime.

191

## 192 Collateral Sensitivity Likelihoods

193 Our experimental results demonstrate that the evolution of antibiotic resistance is non-  
194 repeatable, and that the efficacy of a second-line drug can depend on the specific evolutionary  
195 trajectory that occurs under a first. As such, where a pair of drugs exhibit collateral sensitivity in  
196 a small number of experimental replicates, it need not be the case that collateral sensitivity always  
197 occurs. Rather than give up entirely on the concept of collateral sensitivity between drugs, we  
198 propose that *collateral sensitivity likelihoods* (CSLs) should be derived. By deriving the likelihood  
199 of collateral sensitivity between drugs, we can quantify the risk associated with different drug  
200 sequences. Figure 5(A) shows an example table of collateral sensitivity likelihoods derived from



Replicate	SHV-1 SNVs	Chromosomal SNVs	Deletions (ranges)	IS1D Insertions
Parental		2099555 T>C (intergenic yedK/yedL)		
X1p10			4166399-4177327	
X2p10	G242S			
X3p10	G238C		3079240-3088253	IS1D at 2849873 interrupts CP4-57 prophage predicted protein; 580 bp deletion adjacent
X4p10	G238A		3892703-3903946 2896300-2906979	
X5p10				IS1D at 3506340 interrupts dusB
X6p10	G238A			
X7p10				
X8p10		2401329 T>A (ompC Q144V)		
X9p10				IS1D at 2401801 (upstream of ompC)
X10p10	G238S	3630620 C>A (envZ R339L); 771931 C>T (speF L115L)	4387943-4410705	IS1D at 4410705 interrupts rpiB; 14kb deletion adjacent
X11p10		3630620 C>A (envZ R339L)	2896300-2906979	IS1D at 2906979 interrupts gshA; 12kb deletion adjacent
X12p10	G238S			

**Table 2. Mutations identified through whole genome sequencing.** The single nucleotide variants (SNVs) both within SHV and elsewhere, insertions and deletions identified through whole genome sequencing of the replicates X1-X12 following passage 10 are list.

201 the *in silico* evolution model. We note that whilst there exist 28 drug pairs exhibiting guaranteed  
202 collateral sensitivity ( $p = 1.0$ , right), there also 16 others with likelihood  $1.0 > p \geq 0.75$  of  
203 collateral sensitivity. Where collateral sensitivity is assayed from a small number of experimental  
204 evolution replicates, these drug pairs may appear to exhibit universal collateral sensitivity and  
205 could thus unexpectedly fail stochastically. Conversely, if no universally collaterally sensitive  
206 drugs were known, drug pairs exhibiting a high likelihood of collateral sensitivity might represent  
207 the best option available.

208 Figure 5(B) shows the experimentally derived CSLs for antibiotics administered following  
209 cefotaxime. We find that collateral sensitivity is rare, with  $p = \frac{1}{30}$  for TIC being the most  
210 likely. If we also consider the likelihood that sensitivity of the second-line drug is unchanged,  
211 then it is clear that piperacillin (PIP) or gentamicin (GNT) are the best second-line drugs  
212 following cefotaxime (amongst those we have assayed). Conversely, cross resistance is near  
213 universal in cefazolin (CFZ) and ceftolozane/tazobactam (CFT). For puromycin (PMC) and  
214 ampicillin/sulbactam (SAM), we estimate that cross resistance occurs with probability  $p > 0.5$ ,  
215 but that the probability of no-change or collateral sensitivity is still high ( $p > 0.3$  in both  
216 cases). Drugs such as these highlight the importance of deriving collateral sensitivity likelihoods



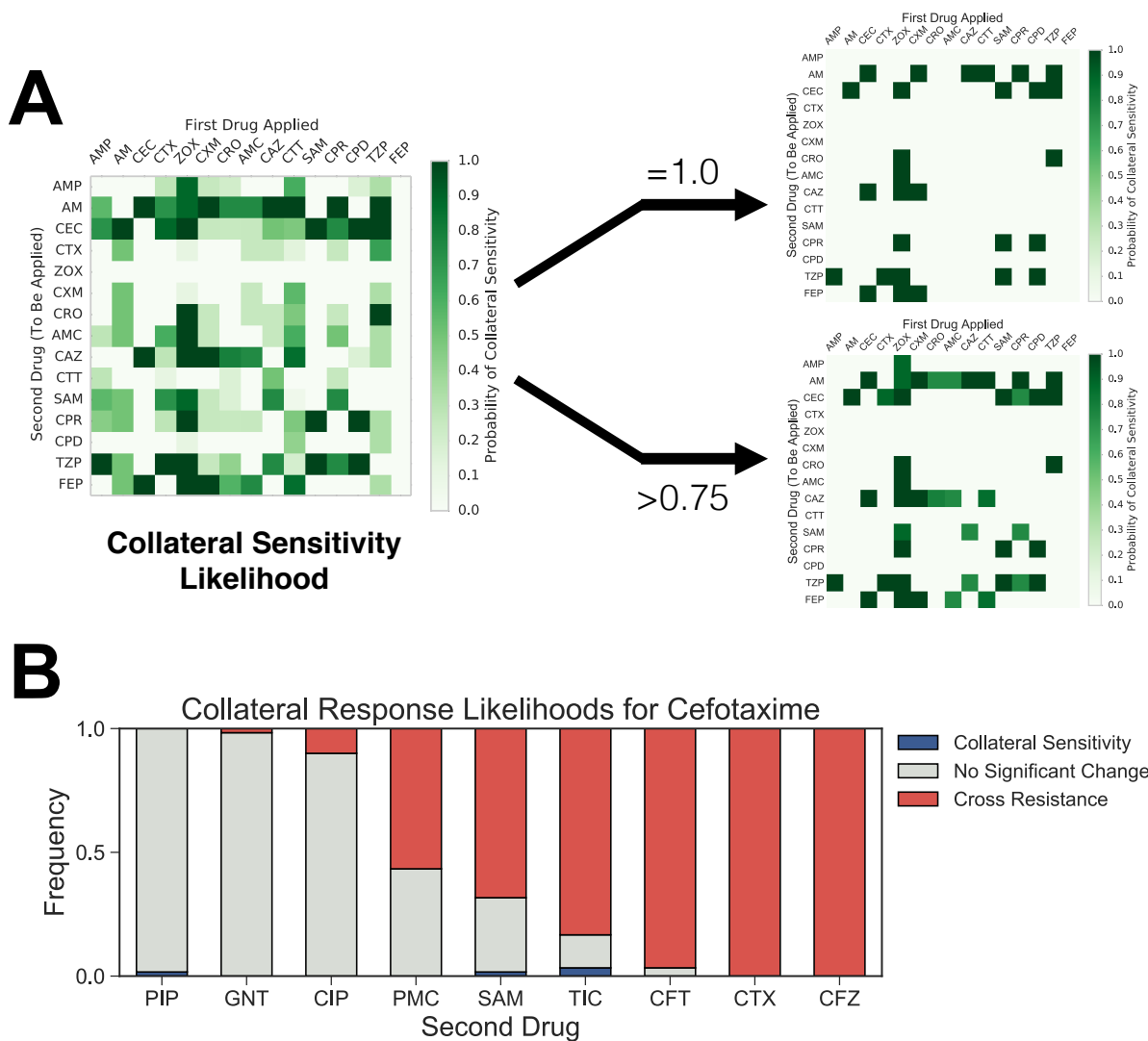


**Figure 5. Collateral sensitivity likelihoods** **A)** (Left) The table of collateral sensitivity likelihoods (CSLs) derived from the mathematical model. Each entry indicates the likelihood that the first drug (rows) induces increased sensitivity in the second (columns). (Right) The CSL table thresholded for drugs with  $p = 1.0$  (top) and  $p \geq 0.75$  (bottom) probability of inducing collateral sensitivity. **B)** The estimated likelihoods for collateral sensitivity, cross resistance or no change in sensitivity derived from the sixty replicates of experimental evolution.

217 by means of multiple evolutionary replicates, as a single evolutionary replicate may identify  
 218 unchanged sensitivity where cross resistance is likely.

219

## 220 Discussion

221 We have demonstrated the existence of an evolutionary branching point in the fitness  
222 landscape of cefotaxime that can induce divergent evolution and differential collateral response to  
223 second-line antibiotics. By means of 60 replicates of experimental evolution, we have estimated  
224 the likelihood of collateral sensitivity in each of 8 second-line therapies. Critically, we find that  
225 collateral sensitivity is never universal, and is in fact rare. Furthermore, by consideration of  
226 a mathematical model of evolution parametrised by small, combinatorially complete fitness  
227 landscapes, we have highlighted the extent and importance of evolutionary divergence. This  
228 modelling highlights that divergent collateral response is likely common (occurring in 14/15 drugs  
229 for which empirical landscapes were derived) and further, that even where collateral sensitivity  
230 is reported from a small number of evolutionary replicates, cross-resistance can still occur with  
231 high likelihood.

232 Taken together, our results indicate that we must take care when interpreting collateral  
233 sensitivity arising in low-throughput evolution experiments. To this end, we propose that collateral  
234 sensitivity likelihoods should be evaluated by use of multiple parallel evolutionary replicates  
235 to better capture the inherent stochasticity of evolution. The high-throughput experimental  
236 evolution necessary to accurately evaluate CSLs between many drug pairs could be facilitated by  
237 automated cell culture systems, such as the morbidostat developed by Toprak et al. [34] which  
238 incorporates automated optical density measurements and drug delivery to track and manipulate.

239 It should be noted that although the evolution of pathological bacteria within the clinic is most  
240 likely stochastic, it is unclear whether the gradient plate system model used in the present study,  
241 and others [14], correctly captures this stochasticity. The gradient plate method proceeds by  
242 serial replating of bacterial populations that induces population bottlenecks and strong selection.  
243 This mode of population dynamics clearly differs from that which *E. coli* experience naturally.  
244 It may be the case that additional stochasticity is introduced as evolutionary phenomena such  
245 as clonal interference, wherein multiple fitter clones compete, do not occur. To empirically  
246 determine collateral sensitivity likelihoods it may be the case that we must employ novel *in vitro*  
247 experimental techniques to more closely match *in vivo* dynamics. Here too, automated culture  
248 systems such as the morbidostat could help, as automated changes to the drug concentration can  
249 prevent the bacterial population expanding too rapidly, mitigating the need for serial replating.

250 The mathematical model we have presented does not capture the full complexity of evo-  
251 lution. For example, we do not account for deletions, insertion of duplications of genes such  
252 as SHV. Nevertheless, this model still proves useful in providing intuition about the extent to  
253 which stochasticity can drive differential collateral response. We can expect the introduction of  
254 additional mutational complexity to introduce further stochasticity. An immediate improvement  
255 to our modelling would be to extend the model to account for alternative population dynamics;  
256 for example, permitting heterogeneous populations, variable population sizes or drug pharmaco-

257 dynamics. A further complication is that drug resistance can arise by physiological adaptations  
258 in addition to genetic mutation, which our mathematical modelling does not take into account.  
259 We see evidence for physiological adaptation in the evolution of the replicate X7 which exhibits  
260 increased resistance to cefotaxime without associated mutations. Further, changes in sensitivity  
261 arising from such phenotypic plasticity may be reversible over short time scales [9]. Ultimately, by  
262 the use of extended mathematical models we may be able to better simulate *in vitro* experiments  
263 in order to understand how generalisable they are to *in situ* evolutionary dynamics [10].

264 As an alternative to high throughput evolutionary experiments, we note that drug sequences  
265 are frequently prescribed in the clinic. Thus, the distributed collection of matched pre- and  
266 post-therapy drug sensitivity assays, potentially coupled with genomic sequencing where this is  
267 feasible, could provide sufficient data to determine CSLs. This approach is particularly appealing  
268 as the CSLs derived would not be subject to the caveats regarding experimentally derived  
269 measures of collateral sensitivities outlined above. Further, clinically derived CSLs would readily  
270 account for non-genetic adaptations and inter-patient variabilities in physiology that may impact  
271 drug sensitivities. A similar approach has already been employed in the treatment of HIV to  
272 monitor the evolution of drug resistance [13, 17].

273 Regardless of the approach taken to derive CSLs, what is clear is that we must move beyond  
274 the present methodology of designing drug sequences through low-replicate-number experimental  
275 evolution, and towards an evolutionarily informed strategy that explicitly accounts for the  
276 inherent stochasticity of evolution.

## 277 **Methods**

### 278 **Mathematical Modelling of Evolution**

279 The probability for evolutionary trajectories through the empirically derived fitness landscapes  
280 were calculated from a previously described mathematical model [23]. Briefly, the population is  
281 assumed to be isogenic and subject to Strong Selection Weak Mutation (SSWM) evolutionary  
282 dynamics. Thus, the population genotype (taken from domain  $\{0, 1\}^4$ ) is modelled as periodically  
283 replaced by a fitter (as determined by the landscape) neighbouring genotype (defined as any  
284 genotype whose Hamming distance from the population genotype is equal to one). This process  
285 is stochastic and the likelihood of a genotype,  $j$ , replacing the present population genotype,  $i$ , is  
286 given by

$$\mathbb{P}(i \rightarrow j) = \begin{cases} \frac{(f(j)-f(i))^r}{\sum_{\substack{g \in \{0,1\}^N, \text{Ham}(i,g)=1 \\ f(g)-f(i)>0}} (f(g)-f(i))^r} & \text{if } f(j) > f(i) \text{ and } \text{Ham}(i, j) = 1 \\ 0 & \text{otherwise} \end{cases} . \quad (1)$$

287 Where no such fitter neighbour exists, the process is terminated. The value of  $r$  determines the  
288 extent to which the fitness benefit of a mutation biases the likelihood that it becomes the next  
289 population genotype. We take  $r = 0$ , corresponding to fixation of the first arising resistance  
290 conferring mutation, but our results are robust to changes in  $r$  (See Supplementary Note for  
291 details).

292 For the simulations of *in vitro* evolutionary experiments, we assume an initial genotype  
293 of  $g_0 = 0000$  and determine the final population genotype by sampling from the model until  
294 termination at a local optimum of fitness, say  $g^*$ . Simulated collateral response was calculated  
295 as the fold difference between  $g_0$  and  $g^*$  in a second fitness landscape.

296 The code used to implement the model, produce the figures and analyse the experimental  
297 data is available upon request and will be made publicly available upon publication.

### 298 **Experimental Adaptation to Cefotaxime**

299 All 60 evolutionary replicates were derived from *E. coli* DH10B carrying phagemid pBC SK(-)  
300 expressing the  $\beta$ -lactamase gene SHV-1 [28]. All evolutionary experiments were performed using  
301 Mueller-Hinton agar.

302 Using a spiral plater, cefotaxime solution was applied to Mueller Hinton (MH) agar plates in a  
303 continuously decreasing volume equivalent to a thousand-fold dilution. *E. coli* DH10B pBCSK(-)  
304  $bla_{\text{SHV-1}}$  colonies were suspended to a concentration of  $7 \log_{10}$  CFU/ml in MH broth. Antibiotic

305 plates were then swabbed along the antibiotic gradient with the bacterial suspension. Plates  
306 were incubated overnight at 37°C. The most resistant colonies, as measured by the distance of  
307 growth along the gradient, were resuspended and used to swab a freshly prepared antibiotic  
308 plate. The process was repeated for a total of 10 passages. The entire experiment was completed  
309 60 times using the same parental strain to generate the cefotaxime resistance replicates X1–X60.

## 310 Determination of Minimum Inhibitory Concentration

311 The minimum inhibitory concentration of each antibiotic was determined for both the parent  
312 strain and the cefotaxime resistant replicates according to guidelines outlined by the Clinical and  
313 Laboratory Standards Institute [5]. MICs were assayed in triplicate as series of 2-fold dilutions.  
314 Where the MIC exceeded the maximum concentration considered, 4096  $\mu\text{g/ml}$ , the precise value  
315 was not determined and a lower bound MIC of  $\geq 8192\mu\text{g/ml}$  was taken.

The MIC was determined from the replicates by maximum likelihood estimation using a statistical model outlined by Weinreich et al. [35]. Briefly, we assume that the  $j^{\text{th}}$   $\log_2$  transformed MIC measurement for the  $i^{\text{th}}$  evolutionary replicate, under the drug  $d$ , denoted  $x_{i,j}^d$ , is determined as

$$x_{i,j}^d = m_i^d + \epsilon_{i,j,d}$$

316 where  $\epsilon_{i,j,d} = +1, 0, -1$  with probability  $p/2, 1 - p, p/2$  respectively. Here, each  $m_i^d$  denotes  
317 the true MIC for the  $i^{\text{th}}$  replicate (with  $i = 0$  denoting the parental line) and  $p$  denotes the  
318 likelihood of measurement error. We assume  $p$  is fixed across technical replicates, evolutionary  
319 replicates and drugs. Note the assumption that we never erroneously take a measurement that  
320 differs from the true MIC by greater than a factor of two. This is justified by noting that in no  
321 instance do the maximum and minimum MICs measured in our analysis differ by greater than  
322  $4\times$  (Supplementary Table X).

Maximum likelihood estimates (mle) for  $m_i^d$  are used as the MICs in our analysis. The likelihood function is given by

$$\mathcal{L}(x_{9=0,1}^1 \cdots x_{60,3}^9 | m_1^1 \cdots m_{60}^9, p) = \prod_{d=1}^9 \prod_{i=0}^{60} \prod_{j=1}^3 \left( (1-p)\delta_{x_{i,j}^d, m_i^d} + \frac{p}{2}\delta_{x_{i,j}^d, m_i^d+1} + \frac{p}{2}\delta_{x_{i,j}^d, m_i^d-1} \right)$$

where  $\delta$  denotes the Kronecker delta function. By observation, the mle for each  $m_i^d$  is given by the median of  $x_{i,1}^d$ ,  $x_{i,2}^d$  and  $x_{i,3}^d$ , except in the case that two of these values are precisely  $4\times$  the other, in which case the mle is the mid-point between the maximum and minimum. Letting  $r$  denote the number of replicate/drug combinations in which all three measurements equal the mle,  $s$  denote the number in which  $2/3$  measurements equal the mle,  $t$  the number in which  $1/3$

equal the mle and  $u$  the number in which 0/3 equal the mle. Then the mle for  $p$  is given by

$$p = \frac{s + 2t + 3u}{3(r + s + t + u)}.$$

323 This identity can be verified by first principles (by taking the derivative of the likelihood function)  
324 but is also quite intuitive - it is simply the proportion of measurements that differ from the  
325 inferred mle for the MIC. In our experiment,  $r = 338$ ,  $s = 196$ ,  $t = 11$  and  $u = 4$ , which yields an  
326 mle for the measurement error rate of  $p = 0.14$ .

327 The full data set, along with the inferred MIC values, are presented in Supplementary Table  
328 1.

### 329 Collateral Sensitivity Analysis and Significance Testing

330 To determine collateral sensitivity (or cross resistance) we determined which evolutionary  
331 replicates exhibited a significantly different MIC from the parental line via a likelihood ratio  
332 test. In total, 60 comparisons were performed for each of the 9 drugs, yielding a total of 540  
333 comparisons. A Bonferroni correction was used to account for multiple hypothesis testing. For  
334 those replicates exhibiting a significant ( $p < 0.05/540$ ) change in MIC, the collateral response  
335 was determined as

$$\text{CR} = m_i^d - m_0^d. \quad (2)$$

336 Otherwise, the set  $\text{CR} = 0$ .

### 337 Targeted Sequencing of SHV

338 Plasmid DNA was isolated using the Wizard Plus Minipreps DNA purification systems (Promega).  
339 Sequencing of the SHV gene was performed using M13 primers (MCLab, Harbor Way, CA).

340

### 341 Whole Genome Sequencing

342 For genome sequencing, total DNA was prepared using MasterPure Complete DNA Purifica-  
343 tion Kit (Epicentre; Madison, Wisconsin). NexteraXT libraries were prepared and sequenced  
344 on an Illumina NextSeq 500 at the Genomics Core at Case Western Reserve University. Paired  
345 sequence reads were mapped using bwa-mem to the DH10B genome (accession CP000948.1), the  
346 pBC SK(-) plasmid (<https://www.novoprolabs.com/vector/V12548>), and the SHV-1 gene (acces-  
347 sion JX268740.1). Reads were also assembled into contigs using velvet [39]. Three approaches  
348 were used to identify *de novo* mutations. First, single-nucleotide variants (SNVs) were called  
349 using the mapped reads using the Genome Analysis Toolkit (GATK) [20]. Second, large deletions

350 were identified using a combination of detection of low-coverage regions of the reference based  
351 on read mapping results and BLAST searches between the DH10B reference sequence and the  
352 contigs. Insertion sequence (IS) elements present in the DH10B genome were identified using  
353 ISfinder [30] and locations for IS elements were mapped in the contigs using ISseeker [1].

## 354 **Data Availability**

355 All MIC measurements are available in Supplementary Table 1. All sequencing data will be  
356 deposited to the NCBI Short read archive upon acceptance for publication.

## 357 **Acknowledgements**

358 DN would like to thank the Engineering and Physical Sciences Research Council (EPSRC) for  
359 generous funding for his doctoral studies (OUCL/DN/2013). JGS is grateful to the NIH for  
360 their generous loan repayment program and to the Paul Calabresi Career Development Award  
361 for Clinical Oncology (NIH K12CA076917). ARAA would like to acknowledge the National  
362 Cancer Institute (NCI) funded Physical Science Oncology Center grant, U54CA193489. This  
363 study was supported in part by funds and facilities provided by the Cleveland Department of  
364 Veterans Affairs, Veterans Affairs Merit Review Program award number 1I01BX001974, from  
365 the Biomedical Laboratory Research & Development Service of the VA Office of Research and  
366 Development and the Geriatric Research Education and Clinical Center VISN 10 to R.A.B. This  
367 work was also supported by funds from the National Institute of Allergy and Infectious Diseases  
368 of the National Institutes of Health under award numbers R01AI063517, R01AI072219, and  
369 R01AI100560 to R.A.B.

370 Funding organizations were not involved in the design and conduct of the study; collection,  
371 management, analysis, and interpretation of the data; and preparation, review, or approval of  
372 the manuscript. The content is solely the responsibility of the authors and does not necessarily  
373 represent the official views of the National Institutes of Health or the Department of Veterans  
374 Affairs.

## 375 **References**

- 376 1. Mark D Adams, Brian Bishop, and Meredith S Wright. Quantitative assessment of insertion  
377 sequence impact on bacterial genome architecture. *Microbial genomics*, 2(7), 2016.
- 378 2. Camilo Barbosa, Vincent Trebosc, Christian Kemmer, Philip Rosenstiel, Robert Beardmore,  
379 Hinrich Schulenburg, and Gunther Jansen. Alternative evolutionary paths to bacterial

- 380 antibiotic resistance cause distinct collateral effects. *Molecular biology and evolution*, 34  
381 (9):2229–2244, 2017.
- 382 3. Jessica MA Blair, Mark A Webber, Alison J Baylay, David O Ogbolu, and Laura JV  
383 Piddock. Molecular mechanisms of antibiotic resistance. *Nature Reviews Microbiology*, 13  
384 (1):42, 2015.
- 385 4. François Clavel and Allan J Hance. HIV drug resistance. *New England Journal of Medicine*,  
386 350(10):1023–1035, 2004.
- 387 5. Clinical and PA Laboratory Standards Institute, Wayne. *Performance standards for*  
388 *antimicrobial susceptibility testing: 22nd informational supplement. CLSI document M100-*  
389 *S22.*, 2012.
- 390 6. Julian Davies and Dorothy Davies. Origins and evolution of antibiotic resistance. *Microbi-*  
391 *ology and Molecular Biology Reviews*, 74(3):417–433, 2010.
- 392 7. Mari Rodriguez de Evgrafov, Heidi Gumpert, Christian Munck, Thomas T Thomsen, and  
393 Morten OA Sommer. Collateral resistance and sensitivity modulate evolution of high-level  
394 resistance to drug combination treatment in *Staphylococcus aureus*. *Molecular Biology*  
395 *and Evolution*, page msv006, 2015.
- 396 8. J Arjan Gm De Visser and Joachim Krug. Empirical fitness landscapes and the predictabil-  
397 ity of evolution. *Nature reviews. Genetics*, 15(7):480, 2014.
- 398 9. Andrew Dhawan, Daniel Nichol, Fumi Kinose, Mohamed E Abazeed, Andriy Marusyk,  
399 Eric B Haura, and Jacob G Scott. Collateral sensitivity networks reveal evolutionary  
400 instability and novel treatment strategies in ALK mutated non-small cell lung cancer.  
401 *Scientific Reports*, 7, 2017.
- 402 10. Samantha E Forde, Robert E Beardmore, Ivana Gudelj, Sinan S Arkin, John N Thompson,  
403 and Laurence D Hurst. Understanding the limits to generalizability of experimental  
404 evolutionary models. *Nature*, 455(7210):220, 2008.
- 405 11. Ayari Fuentes-Hernandez, Jessica Plucain, Fabio Gori, Rafael Pena-Miller, Carlos Reding,  
406 Gunther Jansen, Hinrich Schulenburg, Ivana Gudelj, and Robert Beardmore. Using a  
407 sequential regimen to eliminate bacteria at sublethal antibiotic dosages. *PLoS biology*, 13  
408 (4):e1002104, 2015.
- 409 12. Mel Greaves and Carlo C Maley. Clonal evolution in cancer. *Nature*, 481(7381):306–313,  
410 2012.



- 411 13. Trevor Hinkley, João Martins, Colombe Chappey, Mojgan Haddad, Eric Stawiski, Jean-  
412 nette M Whitcomb, Christos J Petropoulos, and Sebastian Bonhoeffer. A systems analysis  
413 of mutational effects in HIV-1 protease and reverse transcriptase. *Nature Genetics*, 43(5):  
414 487–489, 2011.
- 415 14. Lejla Imamovic and Morten OA Sommer. Use of collateral sensitivity networks to design  
416 drug cycling protocols that avoid resistance development. *Science Translational Medicine*,  
417 5(204):204ra132–204ra132, 2013.
- 418 15. Yunxin J Jiao, Michael Baym, Adrian Veres, and Roy Kishony. Population diversity  
419 jeopardizes the efficacy of antibiotic cycling. *bioRxiv*, page 082107, 2016.
- 420 16. Seungsoo Kim, Tami D Lieberman, and Roy Kishony. Alternating antibiotic treatments  
421 constrain evolutionary paths to multidrug resistance. *Proceedings of the National Academy  
422 of Sciences*, 111(40):14494–14499, 2014.
- 423 17. Roger D Kouyos, Gabriel E Leventhal, Trevor Hinkley, Mojgan Haddad, Jeannette M  
424 Whitcomb, Christos J Petropoulos, and Sebastian Bonhoeffer. Exploring the complexity  
425 of the HIV-1 fitness landscape. *PLoS Genetics*, 8(3):e1002551, 2012.
- 426 18. Viktória Lázár, Gajinder Pal Singh, Réka Spohn, István Nagy, Balázs Horváth, Mónika  
427 Hrtyan, Róbert Busa-Fekete, Balázs Bogos, Orsolya Méhi, Bálint Csörgő, et al. Bacterial  
428 evolution of antibiotic hypersensitivity. *Molecular systems biology*, 9(1):700, 2013.
- 429 19. James Mallet. The evolution of insecticide resistance: have the insects won? *Trends in  
430 Ecology & Evolution*, 4(11):336–340, 1989.
- 431 20. Aaron McKenna, Matthew Hanna, Eric Banks, Andrey Sivachenko, Kristian Cibulskis,  
432 Andrew Kernytsky, Kiran Garimella, David Altshuler, Stacey Gabriel, Mark Daly, et al.  
433 The genome analysis toolkit: a mapreduce framework for analyzing next-generation dna  
434 sequencing data. *Genome research*, 2010.
- 435 21. Portia M Mira, Kristina Crona, Devin Greene, Juan C Meza, Bernd Sturmfels, and Miriam  
436 Barlow. Rational design of antibiotic treatment plans: A treatment strategy for managing  
437 evolution and reversing resistance. *PLoS ONE*, 2015.
- 438 22. Christian Munck, Heidi K Gumpert, Annika I Nilsson Wallin, Harris H Wang, and  
439 Morten OA Sommer. Prediction of resistance development against drug combinations  
440 by collateral responses to component drugs. *Science Translational Medicine*, 6(262):  
441 262ra156–262ra156, 2014.

- 442 23. Daniel Nichol, Peter Jeavons, Alexander G Fletcher, Robert A Bonomo, Philip K Maini,  
443 Jerome L Paul, Robert A Gatenby, Alexander RA Anderson, and Jacob G Scott. Steering  
444 evolution with sequential therapy to prevent the emergence of bacterial antibiotic resistance.  
445 *PLoS Computational Biology*, 11(9):e1004493, 2015.
- 446 24. Tugce Oz, Aysegul Guvenek, Sadik Yildiz, Enes Karaboga, Yusuf Talha Tamer, Nirva  
447 Mumcuyan, Vedat Burak Ozan, Gizem Hazal Senturk, Murat Cokol, Pamela Yeh, et al.  
448 Strength of selection pressure is an important parameter contributing to the complexity of  
449 antibiotic resistance evolution. *Molecular biology and evolution*, 31(9):2387–2401, 2014.
- 450 25. Adam C Palmer, Erdal Toprak, Michael Baym, Seungsoo Kim, Adrian Veres, Shimon  
451 Bershtein, and Roy Kishony. Delayed commitment to evolutionary fate in antibiotic  
452 resistance fitness landscapes. *Nature Communications*, 6:7385, 2015.
- 453 26. Patrick C Phillips. Epistasis—the essential role of gene interactions in the structure and  
454 evolution of genetic systems. *Nature Reviews Genetics*, 9(11):855, 2008.
- 455 27. Frank J Poelwijk, Daniel J Kiviet, Daniel M Weinreich, and Sander J Tans. Empirical  
456 fitness landscapes reveal accessible evolutionary paths. *Nature*, 445(7126):383–386, 2007.
- 457 28. Louis B Rice, Lenore L Carias, Andrea M Hujer, Mary Bonafede, Rebecca Hutton, Claudia  
458 Huyen, and Robert A Bonomo. High-level expression of chromosomally encoded SHV-1  
459  $\beta$ -lactamase and an outer membrane protein change confer resistance to ceftazidime and  
460 piperacillin-tazobactam in a clinical isolate of *Klebsiella pneumoniae*. *Antimicrobial Agents  
461 and Chemotherapy*, 44(2):362–367, 2000.
- 462 29. Jacob Scott and Andriy Marusyk. Somatic clonal evolution: A selection-centric perspective.  
463 *Biochimica et Biophysica Acta (BBA)-Reviews on Cancer*, 1867(2):139–150, 2017.
- 464 30. Patricia Siguier, Jocelyne Pérochon, L Lestrade, Jacques Mahillon, and Michael Chandler.  
465 Isfinder: the reference centre for bacterial insertion sequences. *Nucleic acids research*, 34  
466 (suppl\_1):D32–D36, 2006.
- 467 31. Shingo Suzuki, Takaaki Horinouchi, and Chikara Furusawa. Prediction of antibiotic  
468 resistance by gene expression profiles. *Nature communications*, 5:5792, 2014.
- 469 32. Longzhi Tan, Stephen Serene, Hui Xiao Chao, and Jeff Gore. Hidden randomness between  
470 fitness landscapes limits reverse evolution. *Physical Review Letters*, 106(19):198102, 2011.
- 471 33. Erdal Toprak, Adrian Veres, Jean-Baptiste Michel, Remy Chait, Daniel L Hartl, and Roy  
472 Kishony. Evolutionary paths to antibiotic resistance under dynamically sustained drug  
473 selection. *Nature genetics*, 44(1):101, 2012.

- 474 34. Erdal Toprak, Adrian Veres, Sadik Yildiz, Juan M Pedraza, Remy Chait, Johan Paulsson,  
475 and Roy Kishony. Building a morbidostat: an automated continuous-culture device for  
476 studying bacterial drug resistance under dynamically sustained drug inhibition. *Nature*  
477 *protocols*, 8(3):555, 2013.
- 478 35. Daniel M Weinreich, Nigel F Delaney, Mark A Depristo, and Daniel L Hartl. Darwinian  
479 evolution can follow only very few mutational paths to fitter proteins. *Science*, 312(5770):  
480 111–4, Apr 2006. doi: 10.1126/science.1123539.
- 481 36. Daniel M Weinreich, Nigel F Delaney, Mark A DePristo, and Daniel L Hartl. Darwinian  
482 evolution can follow only very few mutational paths to fitter proteins. *Science*, 312(5770):  
483 111–114, 2006.
- 484 37. Sewall Wright. The roles of mutation, inbreeding, crossbreeding and selection in evolution.  
485 In *Proceedings of the Sixth International Congress on Genetics*, volume 1, pages 356–366,  
486 1932.
- 487 38. Helena Yu, Maria E Arcila, Natasha Rekhtman, Camelia S Sima, Maureen F Zakowski,  
488 William Pao, Mark G Kris, Vincent A Miller, Marc Ladanyi, and Gregory J Riely. Analysis  
489 of mechanisms of acquired resistance to EGFR TKI therapy in 155 patients with EGFR-  
490 mutant lung cancers. *Clinical cancer research*, pages clincanres–2246, 2013.
- 491 39. Daniel Zerbino and Ewan Birney. Velvet: algorithms for de novo short read assembly  
492 using de bruijn graphs. *Genome research*, pages gr–074492, 2008.
- 493 40. Boyang Zhao, Joseph C Sedlak, Raja Srinivas, Pau Creixell, Justin R Pritchard, Bruce  
494 Tidor, Douglas A Lauffenburger, and Michael T Hemann. Exploiting temporal collateral  
495 sensitivity in tumor clonal evolution. *Cell*, 165(1):234–246, 2016.